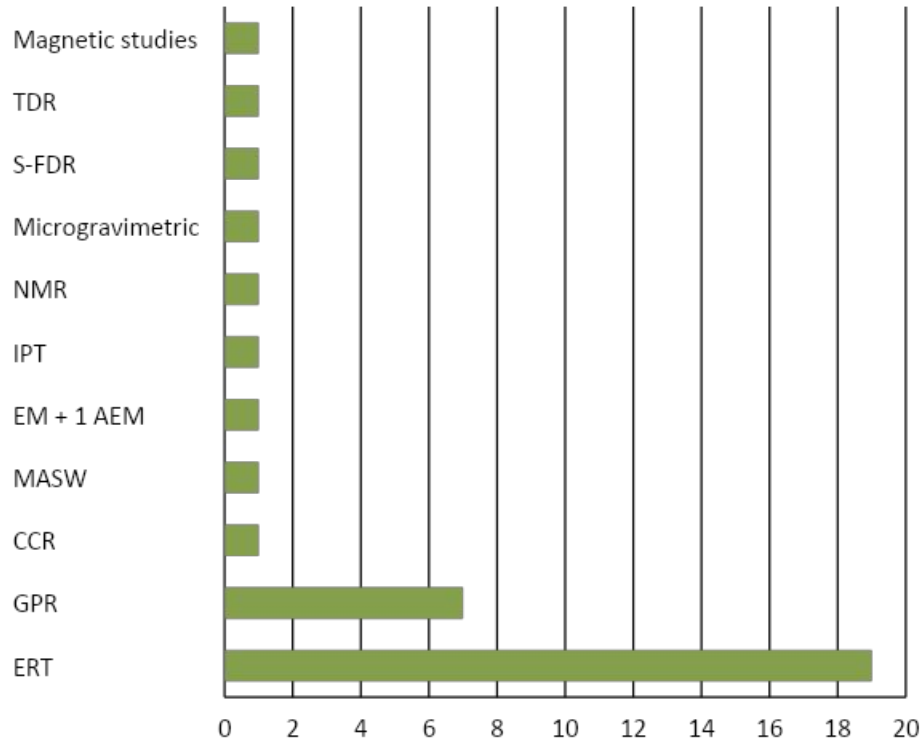


Обзор докладов геофизической сессии на
11й конференции по мерзлотоведению
Потсдам, июнь 2016

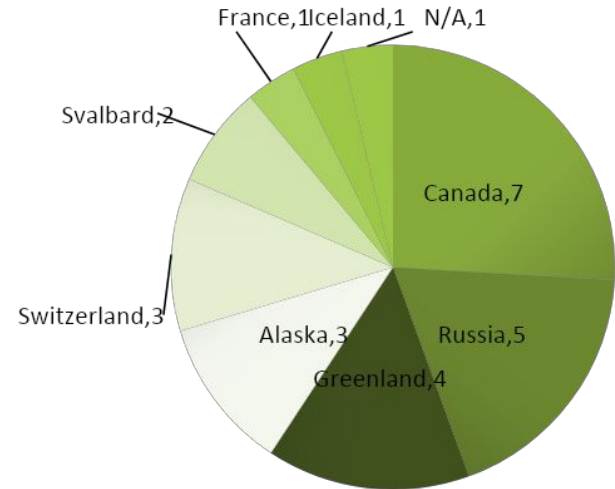
Станиловская Юлия

ОСНОВНОЕ

Методы



- Комбинация методов : ERT + GPR, ERT + seismic, ERT + SP, ERT + RST, ERT + AEM, CCR + GPR, GPR + seismic
- 3D съемка и моделирование
- БУРЕНИЕ



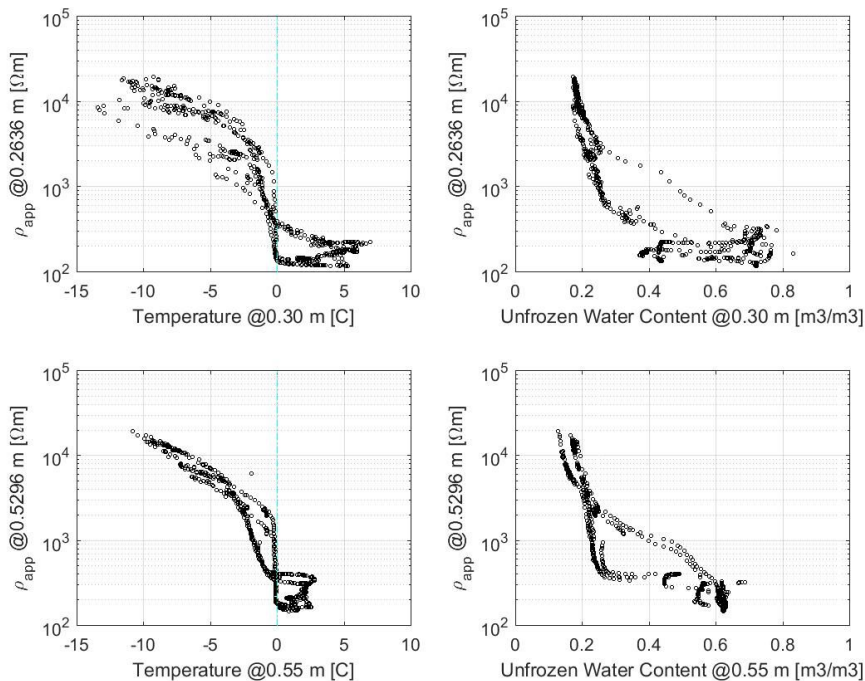
- AEM – Airborne Electromagnetic
- CCR – Capacitively Coupled Resistivity
- EM – Electromagnetic
- ERT – Electrical Resistivity Tomography
- GPR – Ground Penetrating Radar
- IPT – Induced Polarization Tomography
- MASW – Multichannel Analysis Of Surface Waves
- NMR – Nuclear Magnetic Resonance
- RST – Refraction Seismic Tomography
- S-FDR – Spatial Frequency Domain Reflectometry
- SP – Self-Potential Measurements

Долгосрочный мониторинг

17 лет – динамики ледников с использованием ERT в Швейцарии

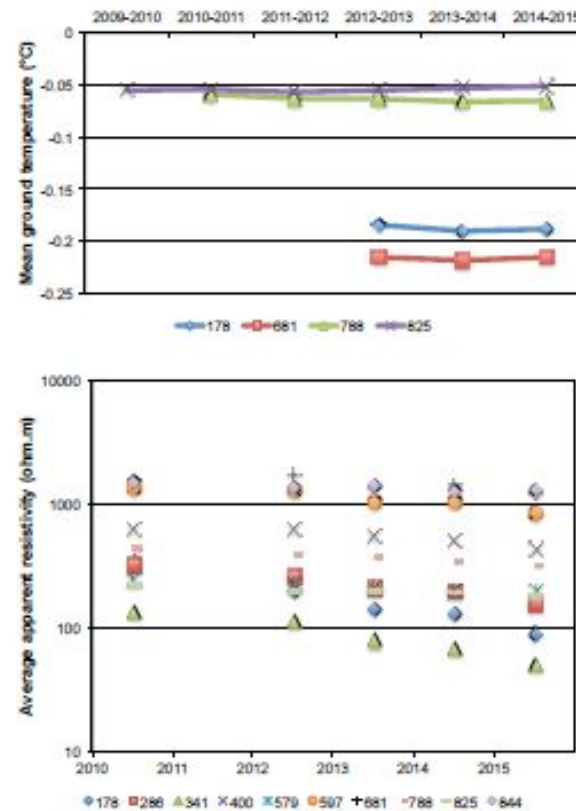
5 лет – динамики сопротивления грунта с использованием ERT в Канаде

3 года – динамики сопротивления грунта с использованием ERT в Гренландии



Daily average resistivity against temperature and water content at two depth levels in the active layer for 3 years

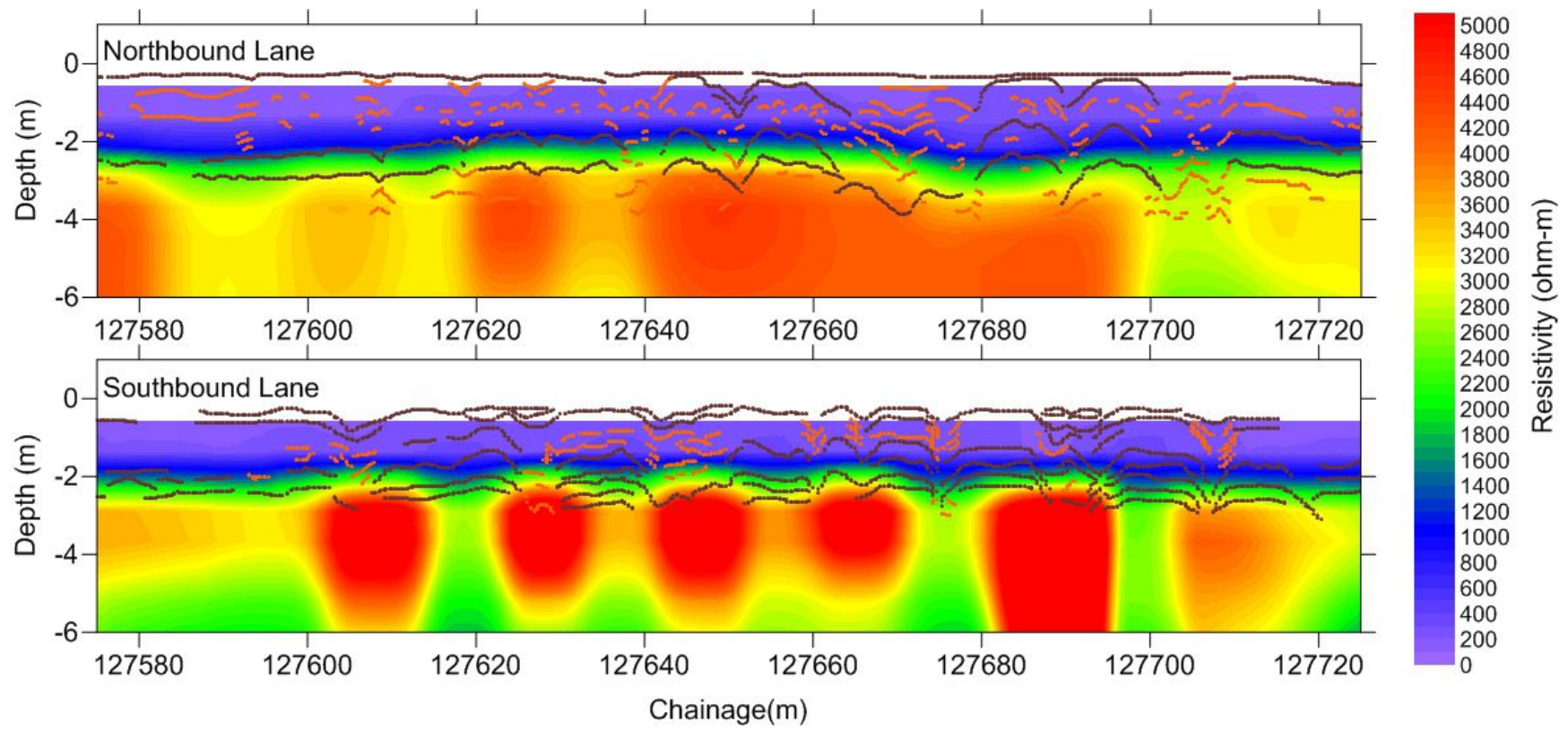
Sonia Tomaskovicova



Time series of ground temperatures (3.75-5 m depths) and average apparent resistivity in August in the Alaska Highway corridor

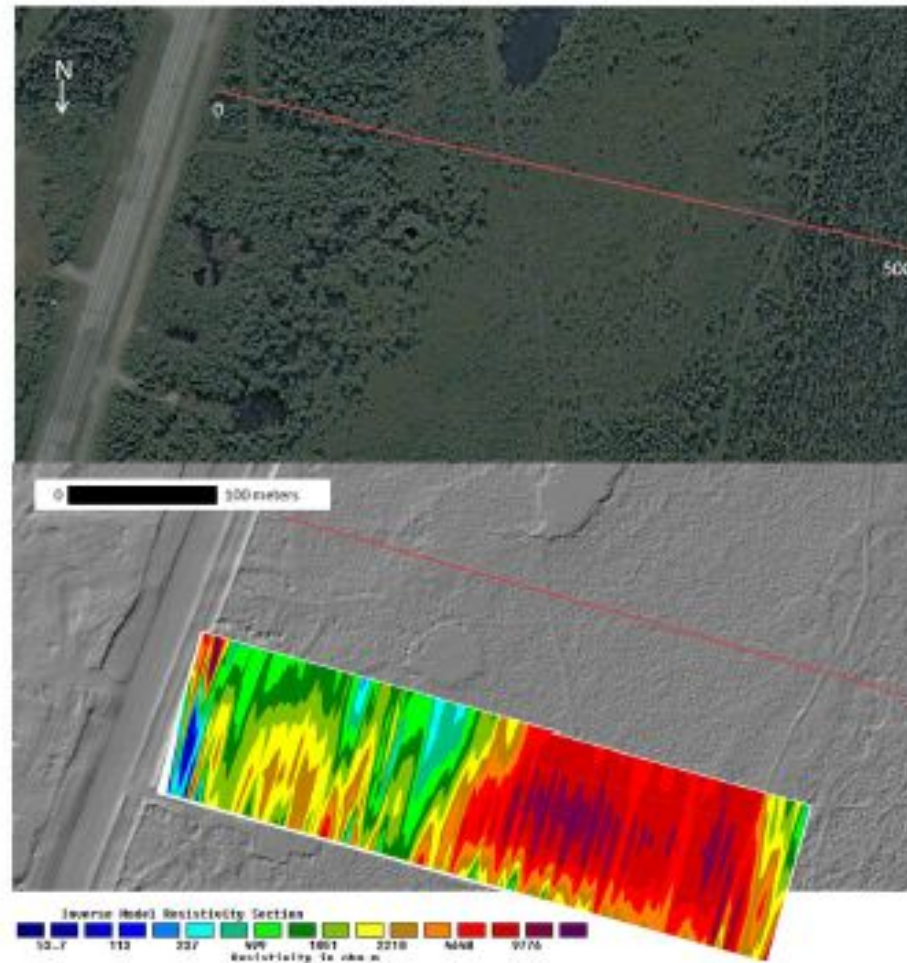
Antoni G. Lewkowicz

Example of CCR and GPR on the Dempster Highway over possible ice-wedge polygons



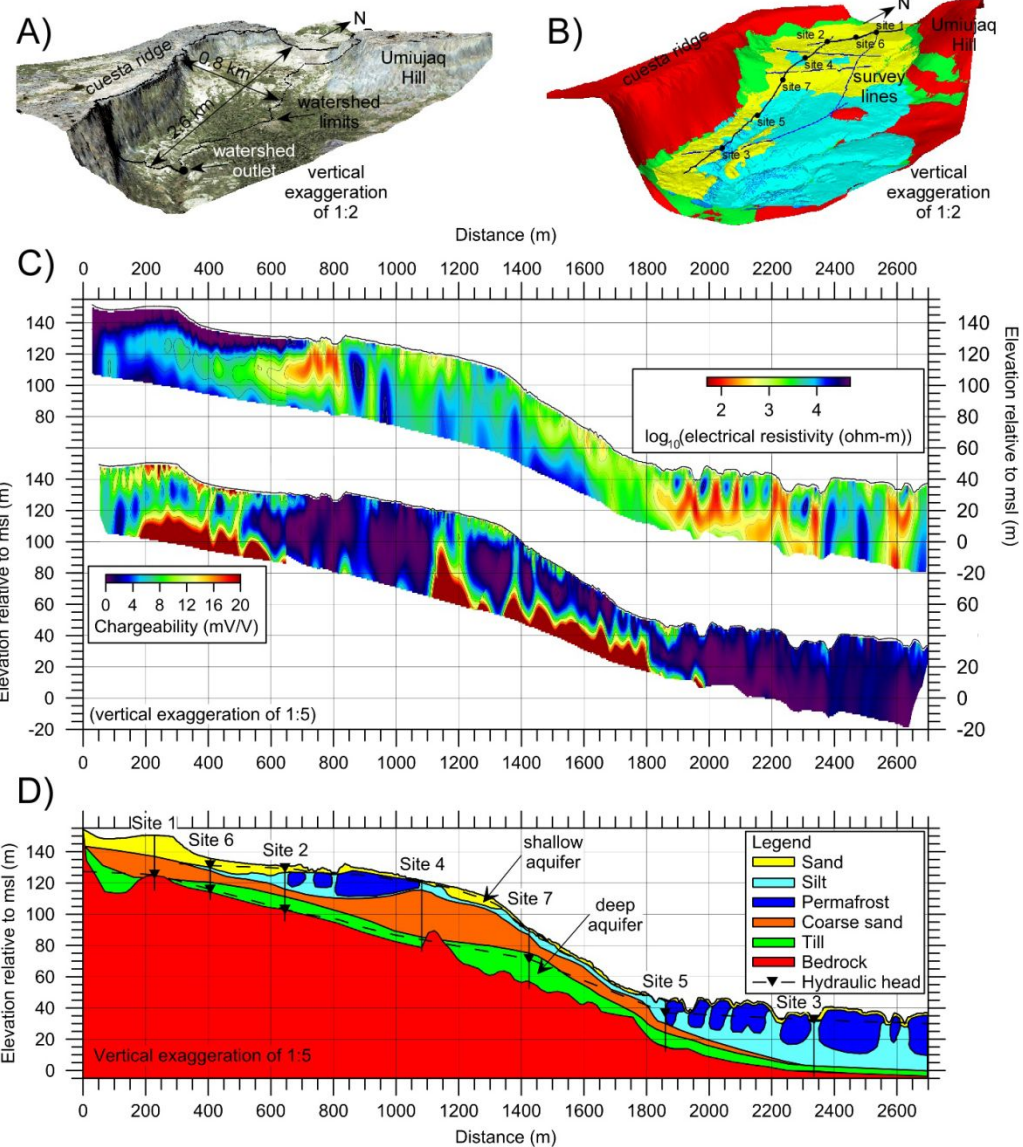
Jane Dawson

A Google Earth image (top) and airborne LiDAR and an electrical resistivity tomography cross section (bottom) from the Farmer's Loop site transect



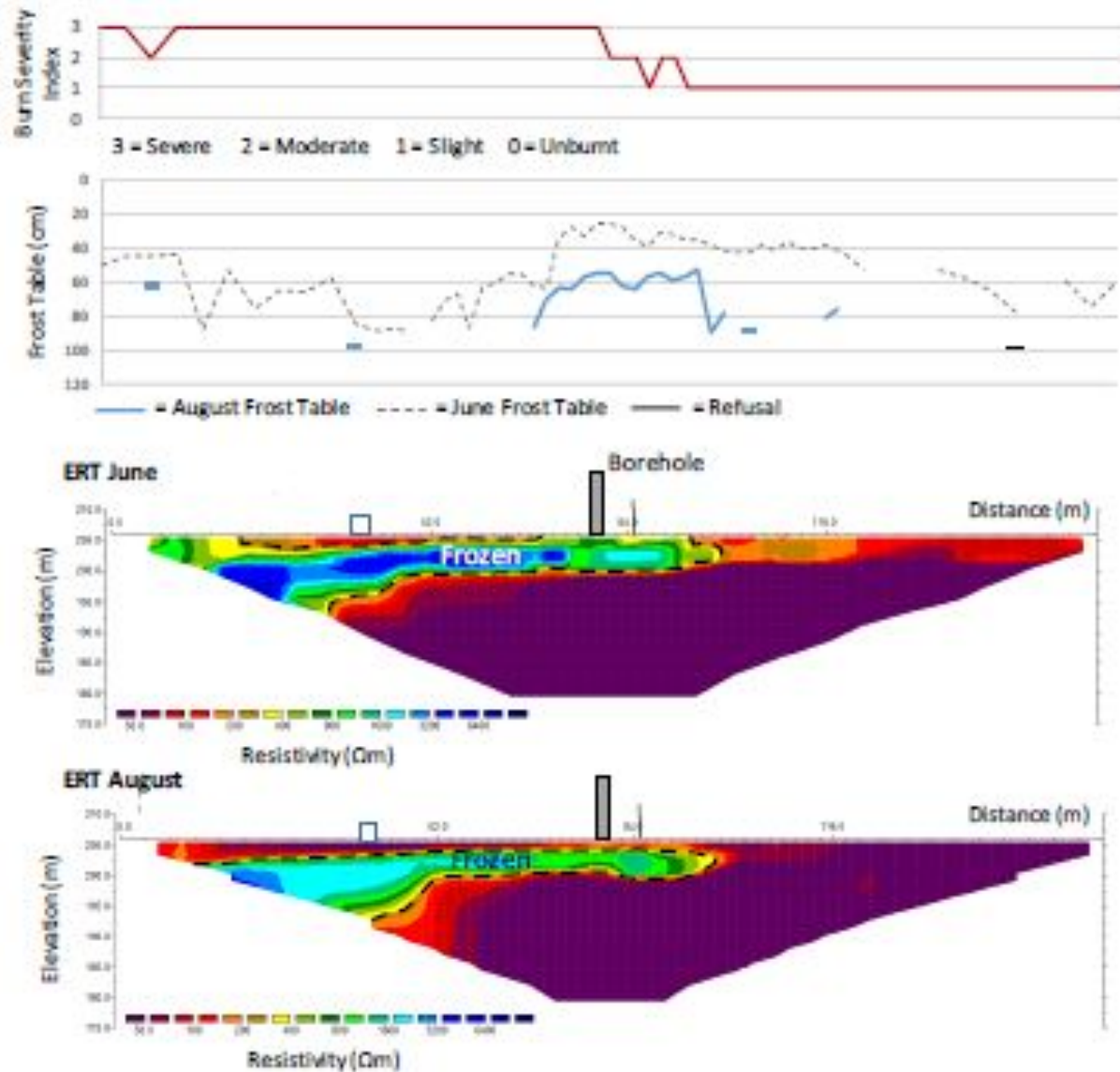
Thomas A. Douglas

- A) Tasiapik valley near Umiujaq
- B) 3D cryohydrogeological model of the studied watershed
- C) Resistivity and chargeability models along the black survey line in B
- D) Cryohydrogeological cross-section assessed from the models in C



Richard Fortier

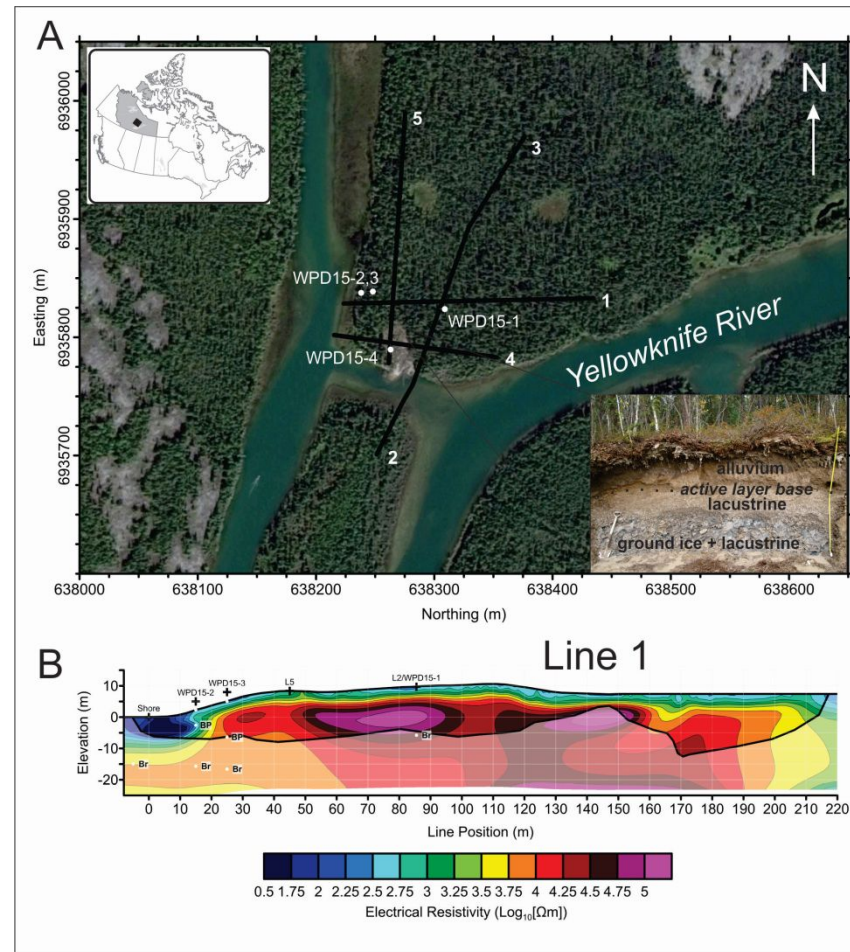
Burn severity, frost table measurements (gaps in data indicates measurements greater than 120cm probe), and resistivity for June and August at a burnt site in the southwestern NWT, Canada



Jean Elizabeth Holloway

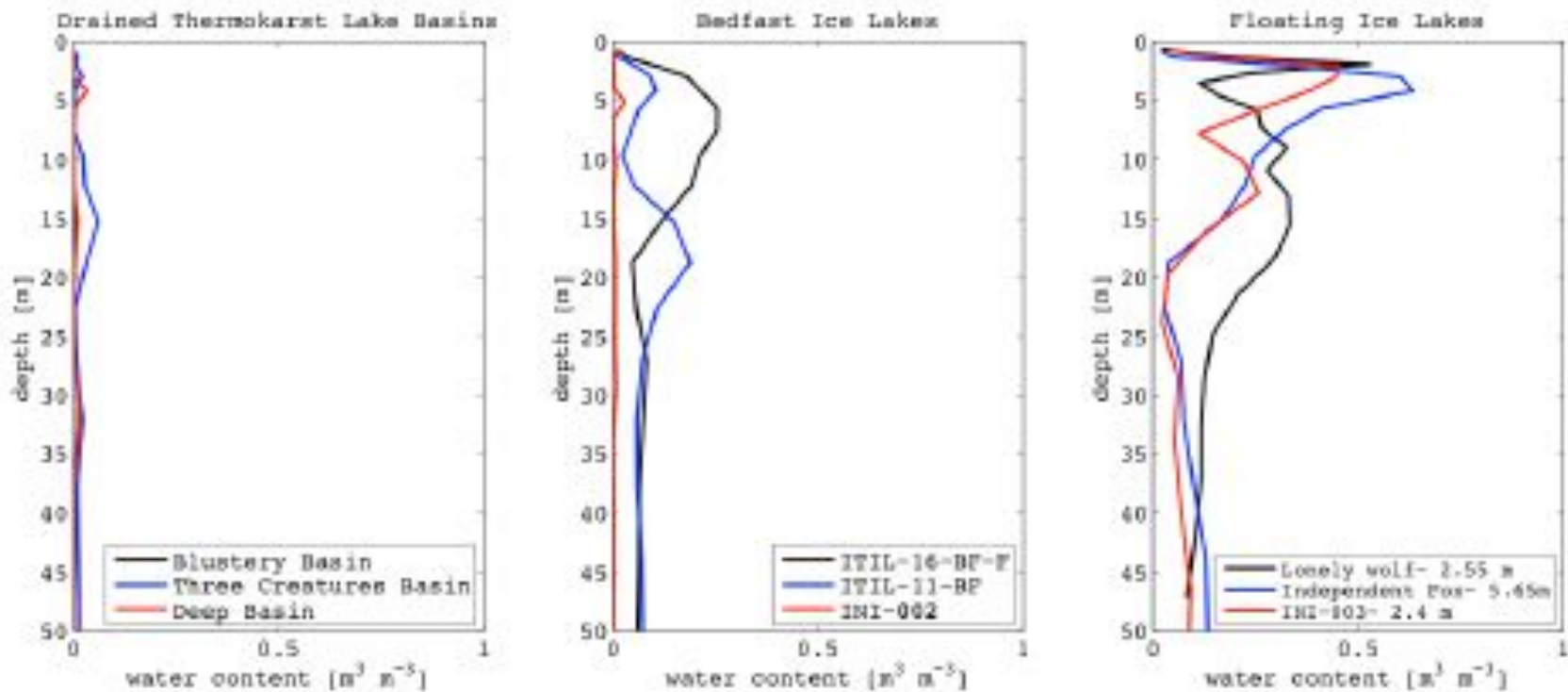
Electrical resistivity survey area and results.

A) Delineation of surveys and boreholes (WPD15-1, 2, 3, 4) conducted within the vicinity of ice-bearing permafrost terrain (see inset) on an island adjacent to the Yellowknife River



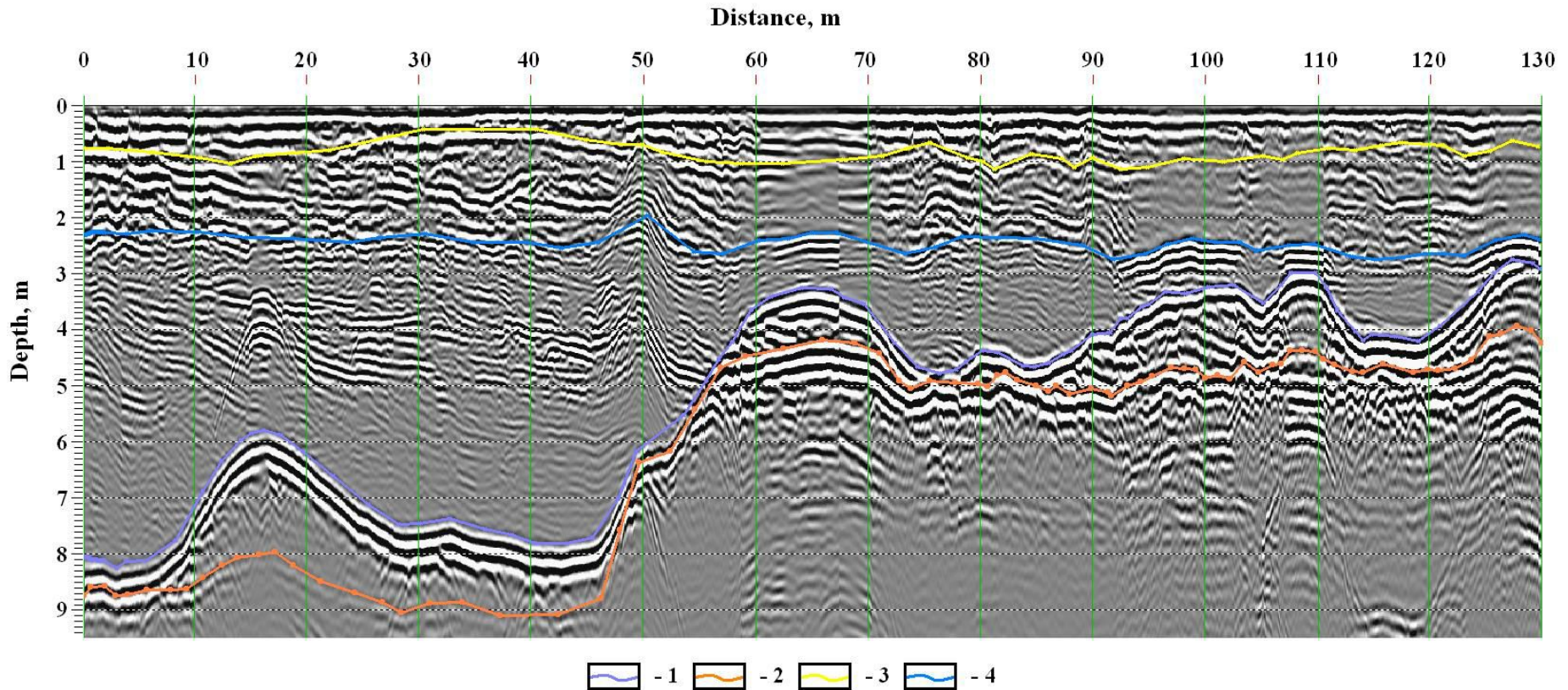
Greg Oldenborger

1D surface nuclear magnetic resonance soundings of talik thaw



Andrew Parsekian

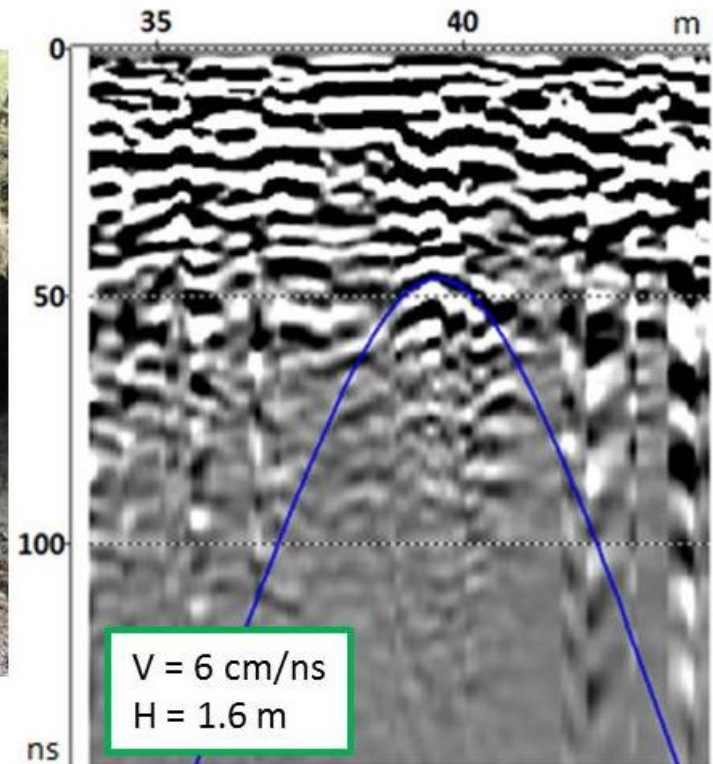
GPR cross section



1 - permafrost table; 2 – boundary in permafrost; 3 – boundary in active layer; 4 – top of water saturated zone

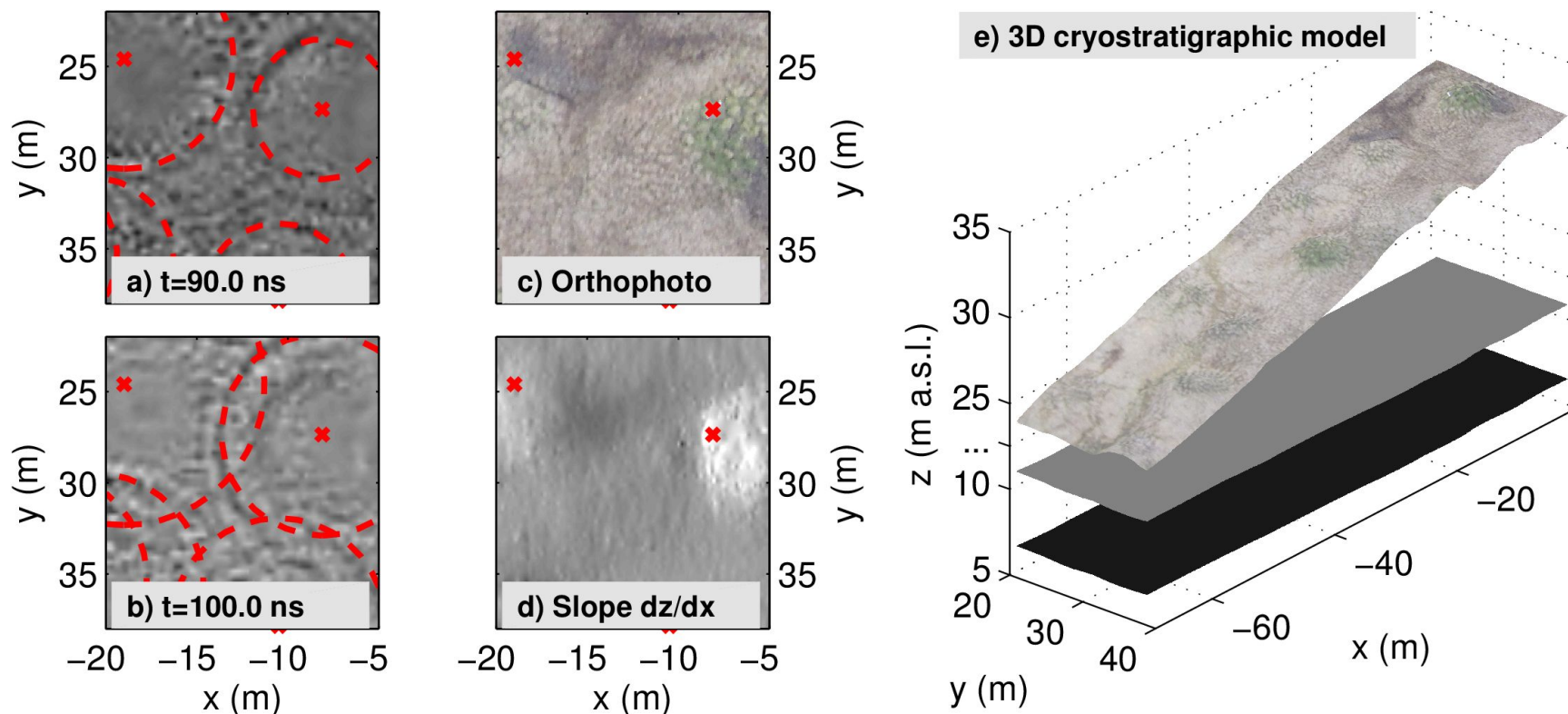
Marat Sadurtdinov

Ice wedge in Chara outcrop and GPR profile over it. The average velocity of the electromagnetic wave in a layer above the ice wedge and calculated depth to it are shown on the GPR profile



Svetlana Bricheva

(a), (b) Two unmigrated time slices showing circular features originating from locations below thermokarst mounds, which are visible on (c), (d). (e) 3D model comprising the base of ice complex strata (grey) and floodplain deposits (black), respectively



Stephan Schennen